



## OPEN ACCESS

## EDITED BY

Ronald M. Bukowski,  
Cleveland Clinic, United States

## REVIEWED BY

Guru P. Sonpavde,  
Dana–Farber Cancer Institute,  
United States  
Carlo Maria Scornajenghi,  
Umberto 1 Hospital, Italy  
Vincenzo Asero,  
Consultant, Italy

## \*CORRESPONDENCE

Shaista Hafeez  
shaista.hafeez@icr.ac.uk

## SPECIALTY SECTION

This article was submitted to  
Genitourinary Oncology,  
a section of the journal  
Frontiers in Oncology

RECEIVED 04 June 2022

ACCEPTED 29 September 2022

PUBLISHED 14 November 2022

## CITATION

Hafeez S, Koh M, Jones K, Ghzal AE,  
D'Arcy J, Kumar P, Khoo V,  
Lalondrelle S, McDonald F,  
Thompson A, Scurr E, Sohaib A and  
Huddart RA (2022) Diffusion-weighted  
MRI to determine response and long-  
term clinical outcomes in muscle-  
invasive bladder cancer following  
neoadjuvant chemotherapy.  
*Front. Oncol.* 12:961393.  
doi: 10.3389/fonc.2022.961393

## COPYRIGHT

© 2022 Hafeez, Koh, Jones, Ghzal,  
D'Arcy, Kumar, Khoo, Lalondrelle,  
McDonald, Thompson, Scurr, Sohaib  
and Huddart. This is an open-access  
article distributed under the terms of  
the [Creative Commons Attribution  
License \(CC BY\)](https://creativecommons.org/licenses/by/4.0/). The use, distribution  
or reproduction in other forums is  
permitted, provided the original  
author(s) and the copyright owner(s)  
are credited and that the original  
publication in this journal is cited, in  
accordance with accepted academic  
practice. No use, distribution or  
reproduction is permitted which does  
not comply with these terms.

# Diffusion-weighted MRI to determine response and long-term clinical outcomes in muscle-invasive bladder cancer following neoadjuvant chemotherapy

Shaista Hafeez<sup>1,2,3\*</sup>, Mu Koh<sup>1,4</sup>, Kelly Jones<sup>1,2</sup>, Amir El Ghzal<sup>1,2</sup>, James D'Arcy<sup>1</sup>, Pardeep Kumar<sup>2</sup>, Vincent Khoo<sup>2,3</sup>, Susan Lalondrelle<sup>1,3</sup>, Fiona McDonald<sup>1,3</sup>, Alan Thompson<sup>2</sup>, Erica Scurr<sup>4</sup>, Aslam Sohaib<sup>4</sup> and Robert Anthony Huddart<sup>1,2,3</sup>

<sup>1</sup>Division of Radiotherapy and Imaging, The Institute of Cancer Research, London, United Kingdom, <sup>2</sup>Urology Unit, The Royal Marsden National Health Service (NHS) Foundation Trust, London, United Kingdom, <sup>3</sup>Department of Radiotherapy, The Royal Marsden NHS Foundation Trust, London, United Kingdom, <sup>4</sup>Department of Diagnostic Radiology, The Royal Marsden National Health Service (NHS) Foundation Trust, London, United Kingdom

**Objective:** This study aims to determine local treatment response and long-term survival outcomes in patients with localised muscle-invasive bladder cancer (MIBC) patients receiving neoadjuvant chemotherapy (NAC) using diffusion-weighted MRI (DWI) and apparent diffusion coefficient (ADC) analysis.

**Methods:** Patients with T2–T4aN0–3M0 bladder cancer suitable for NAC were recruited prospectively. DWI was performed prior to NAC and was repeated following NAC completion. Conventional response assessment was performed with cystoscopy and tumour site biopsy. Response was dichotomised into response (<T2) or poor response (≥T2). Patients proceeded to either radical cystectomy or chemo-radiotherapy as standard of care. Tumour ADC values were calculated for all b-values (ADC<sub>all</sub>) and high b-values (ADC<sub>b100</sub>). Mean ADC, percentiles, skew, kurtosis, and their change (ΔADC and %ΔADC) were determined. Threshold predictive of response with highest specificity was ascertained using receiver operating characteristic (ROC) analysis. Median overall survival (OS), bladder-cancer-specific survival (bCSS), progression-free survival (PFS), and time to cystectomy were estimated using Kaplan–Meier method. Significant area under the curve (AUC) cut points were used to determine relationship with long-term endpoints and were compared using log-rank test.

**Results:** Forty-eight patients (96 DWI) were evaluated. NAC response was associated with significant increase in mean ΔADC and %ΔADC compared to poor response (ΔADC<sub>all</sub> 0.32×10<sup>−3</sup> versus 0.11×10<sup>−3</sup> mm<sup>2</sup>/s; p=0.009, and %ΔADC<sub>all</sub> 21.70% versus 8.23%; p=0.013). Highest specificity predicting response was seen at 75th percentile ADC (AUC, 0.8; p=0.01). Sensitivity,

specificity, positive predictive power, and negative predictive power of  $\% \Delta \text{ADC}_{b100}$  75th percentile was 73.7%, 90.0%, 96.6%, and 52.9%, respectively.  $\% \Delta \text{ADC}_{b100}$  75th percentile  $>15.5\%$  was associated with significant improvement in OS (HR, 0.40; 95% CI, 0.19–0.86;  $p=0.0179$ ), bCSS (HR, 0.26; 95% CI, 0.08–0.82;  $p=0.0214$ ), PFS (HR, 0.16; 95% CI, 0.05–0.48;  $p=0.0012$ ), and time to cystectomy (HR, 0.19; 95% CI, 0.07–0.47;  $p=0.0004$ ).

**Conclusions:** Quantitative ADC analysis can successfully identify NAC response and improved long-term clinical outcomes. Multi-centre validation to assess reproducibility and repeatability is required before testing within clinical trials to inform MIBC treatment decision making.

**Advances in knowledge:** We successfully demonstrated that measured change in DWI can successfully identify NAC response and improved long-term survival outcomes.

#### KEYWORDS

muscle invasive bladder cancer (MIBC), neoadjuvant chemotherapy, MRI, diffusion weighted magnetic resonance imaging (DWI), imaging biomarkers

## Introduction

Curative treatment options for patients with localised muscle-invasive bladder cancer (MIBC) includes either radical cystectomy or radiotherapy delivered with systemic radiosensitisation (1–4). Neo-adjuvant cisplatin-based combination chemotherapy is offered to patients prior to radical treatment given improved overall survival benefit (5, 6). Accurate prediction of neo-adjuvant chemotherapy (NAC) response is required to avoid delays in the effective treatment of potential non-responding tumours. Consensus molecular classification of MIBC has identified six subtypes, which differ in oncogenic mechanism, histological characteristics, and clinical outcomes (7). Despite this, no molecular biomarkers have yet been identified, successfully validated, and prospectively tested to predict NAC response such that they could be routinely applied clinically to inform patient stratification (8).

Imaging biomarkers are used in cancer detection, characterisation, and response assessment (9). In bladder cancer, multi-parametric MRI (mpMRI) has been evaluated for local staging in three meta-analyses (10–12). Performance of mpMRI exceeds both CT imaging and trans-urethral resection of the bladder tumour (TURBT) (13–16). A qualitative mpMRI scoring system, the Vesical Imaging-Reporting and Data System (VI-RADS) for newly diagnosed bladder tumours as seen on T2-weighted sequences, diffusion-weighted imaging (DWI), and dynamic contrast enhancement (DCE) images has been developed (17). However, quantitative analysis may provide additional insights to bladder tumour characteristics (18, 19).

DWI contrast is dependent on the inhibitory effect of cell membranes to the random motion of water molecules. The higher cellular density of tumours restricts water molecule diffusion compared to normal tissues. These diffusion characteristics can be captured quantitatively by several metrics; most commonly the mean apparent diffusion coefficient value (ADC) is used. ADC measurements have association with pathological features that can distinguish between bladder T stage, tumour grade, size, and biological proliferation markers (19–23).

Change in ADC has been used to assess treatment response in other tumours (24–28). Following successful treatment, a decrease in cellularity at the tumour site results in ADC increase. Conventional local bladder treatment response assessment is with cystoscopy. DWI, therefore, has potential for non-invasive local bladder treatment response assessment (23, 29). In this study, we evaluated the role of quantitative DWI analysis to assess local treatment response and long-term survival outcomes for MIBC patients receiving NAC.

## Materials and methods

### Study population

This is a pooled exploratory analysis of patients recruited prospectively to single-centre clinical research and ethics-committee-approved protocol conducted in accordance with Good Clinical Practice guidelines.

All patients had initial TURBT and pathological confirmation of MIBC, and were staged with CT scan of the chest, abdomen, and pelvis. Those with T2-T4aN0-3M0 disease according to the American Joint Committee on Cancer (7th edition) of any histological subtype scheduled to receive NAC were considered eligible if they had no contradiction to MRI or objection to follow-up that included repeat MRI and cystoscopy with biopsy.

## Treatment and conventional response assessment

Suitable patients received platinum combined with NAC. NAC response assessment was made with repeat cystoscopy and bladder tumour site biopsy within 21 days of completing NAC. Radiological evaluation with CT and/or MRI (qualitative interpretation) was also used to support clinical decision-making for patients with extra-vesical or nodal involvement. Conventional local response was assessment dichotomised into response ( $<T2$ ) and poor response ( $\geq T2$ ) (Supplementary Table S1) (30).

Definitive radical treatment decision following NAC, i.e., radical cystectomy or chemo-radiotherapy to the bladder +/- pelvic lymph nodes was made as per standard clinical practice in accordance with national guidelines based on specialist urology multi-disciplinary team review (4).

## MRI protocol

Initial MRI scan was performed following TURBT and prior to cycle 1 NAC. MRI was repeated within 14 days of completing NAC chemotherapy and prior to scheduled cystoscopy and tumour site biopsy.

All patients were examined on a 1.5-T MR scanner using a four-channel sensitivity encoding body coil for anatomic coverage of the pelvis. Bladder distention was achieved by instructing patient to void, drink 350 ml water, and imaging 30 min later. Antispasmodic hyoscine butyl bromide (20mg) was administered intramuscularly before image acquisition to reduce motion artefact from bowel peristalsis (31).

Morphological imaging was performed with axial T1-weighted (T1W) and T2-weighted (T2W) sequences. DWI imaging was performed with an axial free-breathing single-shot echo-planar technique with parallel imaging and spectral adiabatic inversion-recovery fat suppression. Diffusion gradients with b-values of 0, 100, 150, 250, 500, and 750  $s/mm^2$  were applied in three orthogonal directions.

Three different 1.5-T systems were commissioned over the study recruitment period and included Intera (Philips, Best, Netherlands) between 2007 and 2011, Avanto (Siemens Medical Systems, Erlangen, Germany) from 2011 to present,

and Aera (Siemens Medical Systems, Erlangen, Germany) from 2011 to present. Aggregated analysis between the systems was deemed acceptable from phantom-based quality assurance testing (personal communication). All patients scanned on one vendor-specific scanner were re-imaged on the same scanner wherever possible. Imaging parameters used are summarised in Supplementary Table S2. Inter-scanning comparison is provided in the Supplementary Material.

## DWI evaluation and ADC analysis

DWI analysis was performed on masked data by a single investigator (SH) blinded to the pathological response using dedicated IDL-based software (ADEPT; The Institute of Cancer Research, London, UK). A region of interest (ROI) within the bladder was delineated using a computer-assisted segmentation technique identifying the area of greatest impeded diffusion on  $b750s/mm^2$  DWI corresponding to the tumour. The ROI was delineated on every  $b750s/mm^2$  DWI slice where the lesion appeared. Multi-focal tumours within the bladder were planned to be contoured individually given the possibility of a differential lesion response to NAC.

ROI drawn on the 750  $s/mm^2$  image was transferred to the corresponding ADC map to calculate ADC at all six b-values (0, 50, 100, 250, 500, and 750  $s/mm^2$ ), i.e.,  $ADC_{all}$ , and high b-values ( $b100$ , 250, 500, and 750  $s/mm^2$ ), i.e.,  $ADC_{b100}$ , which is perfusion insensitive. This was calculated by fitting pixel-wise mono-exponential model using the following equation,  $S=S_0 e^{-b \cdot ADC}$ , where S is the averaged signal intensity and  $S_0$  is the signal without diffusion weighting.

Individual pixel ADC values through the entire ROI for both  $ADC_{all}$  and  $ADC_{b100}$  was calculated. The mean, 10th, 25th, 50th, 75th, and 90th percentiles, skew, and kurtosis parameters for  $ADC_{all}$  and  $ADC_{b100}$  were derived from histogram (bin width,  $1 \times 10^{-6} mm^2/s$ ) analysis.

## Study objective

The study objective was to determine the association of pre-treatment ADC, post-treatment ADC,  $\Delta ADC$ , and  $\% \Delta ADC$  with conventional tumour response and long-term survival outcomes in patients receiving NAC.

## Statistical considerations

Evaluable patients were defined as those who had baseline and response MRI acquired in accordance with the protocol and received at least one cycle of NAC. If no abnormal DWI signal was measurable on baseline MRI, i.e., patient had achieved complete functional response following TURBT, the proposed

analysis was not possible, and the patient was deemed non-evaluable.

Patient characteristics were reported using descriptive statistics. Statistical analysis was performed using the above ADC histogram-derived features at ADC<sub>all</sub> and ADC<sub>b100</sub>. Absolute change in ADC ( $\Delta$ ADC) following treatment was calculated as the difference between post-treatment and baseline ADC. The relative percentage change in (% $\Delta$ ADC) was also calculated as  $\% \Delta \text{ADC} = (\text{post-NAC ADC} - \text{pre-NAC ADC}) / \text{pre-NAC ADC} \times 100$ .

The association between conventional treatment response with pre-treatment ADC, post-treatment ADC,  $\Delta$ ADC, and % $\Delta$ ADC was analysed using non-parametric tests (Mann-Whitney U and Wilcoxon two sample tests). Where comparison between multiple groups was performed, Kruskal-Wallis analysis was used. Significance values were adjusted for multiple testing (Bonferroni correction).

Receiver operating characteristic (ROC) curve analysis was used to identify threshold predictive of treatment response with the highest specificity. ROC analysis for response status was performed using mean ADC, percentile, skew, and kurtosis for values derived from baseline image, post-treatment image,  $\Delta$ ADC, and % $\Delta$ ADC. The parameter associated with an area under the curve (AUC) >0.6 and p <0.05 was considered significant.

ROC curve cut-point values for significant parameters was found by applying the Youden index *J*, defined as:  $J = \max(\text{sensitivity}_c + \text{specificity}_c - 1)$ , where *c* ranges over all possible criterion values. The sensitivity, specificity, positive predictive value (PPV), and negative predictive value (NPV) of the cut point were determined.

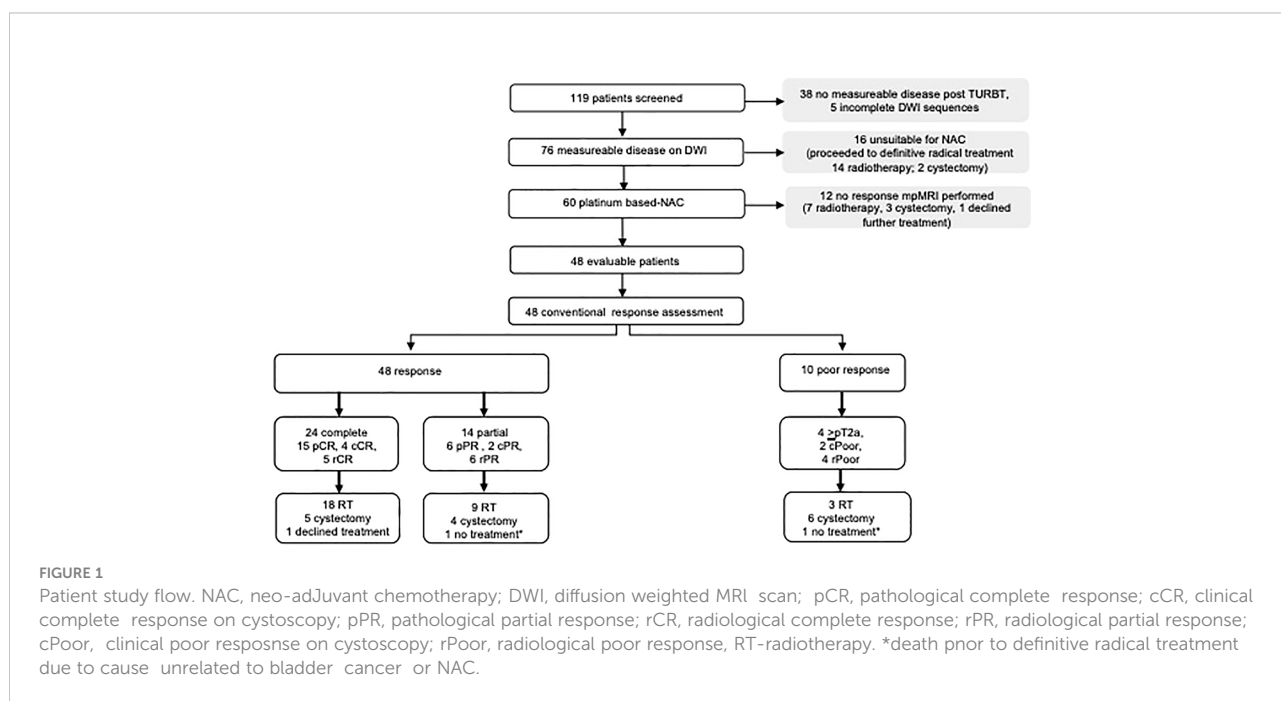
Median overall survival (OS), bladder-cancer-specific survival (bCSS), progression-free survival (PFS), and time to cystectomy were estimated using the Kaplan–Meier method. OS was defined as time from date of NAC start to date of death from any cause. bCSS was defined from NAC start to death due to bladder cancer; patients who died from other or unverified causes were censored at death. PFS was defined as the interval from NAC initiation to disease relapse not amenable to radical salvage. Time to cystectomy was defined from NAC start to date of operation. Surviving patients, progression free, and those with an intact bladder or lost to follow-up were censored at last follow-up.

Significant AUC cut points were used to dichotomise the patient population to determine the potential relationship with long-term endpoints. A comparison between the curves was made with log-rank test. Analyses were carried using SPSS v.22 (IBM, Chicago, Ill., USA) and MedCalc Version 16.4.3 (Medcalc software Ltd, Ostend, Belgium).

## Results

### Patient characteristics

Between September 2007 and August 2013, 119 patients were screened. Forty-eight patients (40%) were available for analysis. Thirty-eight patients (32%) who had no visible abnormality on DWI post TURBT, 17 patients (14%) who had MRI acquisition that deviated from the protocol, and 16 (13%) who proceeded directly to radical treatment without NAC were excluded. Patient study flow is shown in Figure 1.



Patient and tumour characteristics are presented in Table 1. All patients had predominant urothelial histology and unifocal bladder tumours. The median time from diagnostic TURBT to baseline MRI scan was 35 days (range, 8–110 days). A total of 85.4% (41/48) of the patients completed NAC as planned. Cystoscopic evaluation of NAC response was performed in 69% (33/48) of the patients; 52% (25/48) also underwent tumour site biopsy. The remaining patients (31%, 15/48) had radiological NAC response assessment only. Seventy-nine percent (38/48) of the patients demonstrated NAC response.

TABLE 1 Patient and tumour characteristics.

Age	Median years of 69.5 (range, 41–84)
<b>Gender</b>	
Male	40
Female	8
<b>Stage of the primary</b>	
T2	21
T3	21
T4	6
<b>Highest stage</b>	
T2	20
T3	17
T4	5
N+	6
<b>Chemotherapy protocol</b>	
Gemcitabine–Cisplatin*	42
Gemcitabine–Carboplatin	6
<b>Number of cycles (median)**</b>	4 (range 1–6)
<b>Conventional assessment</b>	
Cystoscopy ± biopsy	33
Radiology alone	15
<b>Conventional response</b>	
Complete	24
Partial	14
Poor	10
<b>Definitive treatment</b>	
Radiotherapy (with radiosensitisation)*	30 (18)
Cystectomy	15
No further treatment following neo-adjuvant chemotherapy	3

NAC, neo-adjuvant chemotherapy.

\*Three patients started gemcitabine–cisplatin but were switched to gemcitabine–carboplatin, two because of renal impairment and one because of cardiac co-morbidity.

\*\*Forty-one of the 48 patients completed their planned course of NAC.

One patient stopped after cycle 1 because of symptomatic disease progression, one patient stopped at cycle 1.5 (out of planned three cycles) following a stroke, one patient stopped at cycle 2 (out of planned three cycles) because of duodenal perforation, one patient stopped at cycle 3 (out of planned six) because of poor interval response, one patient stopped at cycle 5 (out of planned six cycles) because of deteriorating renal function, one patient stopped at cycle 5 (out of planned six cycles) because of patient choice, one patient stopped at cycle 5 (out of planned six cycles) because death due to cause unrelated to disease or treatment.

\*Eighteen patient received radiosensitisation with concurrent chemotherapy (17 patients received mitomycin C and 5FU; 1 patient received gemcitabine).

## Response evaluation using DWI change

All tumours seen on T2W were also identified on b750s/mm<sup>2</sup> DWI. The median DWI bladder lesion volume prior to NAC was 7.62 cm<sup>3</sup> (range, 0.34–139.92). Median baseline tumour ADC<sub>all</sub> mean and ADC<sub>b100</sub> mean were 1.35×10<sup>-3</sup> mm<sup>2</sup>/s (range, 0.85–2.04×10<sup>-3</sup>) and 1.22×10<sup>-3</sup> mm<sup>2</sup>/s (range 0.78–1.86×10<sup>-3</sup>) (p<0.001) respectively.

ADC histogram characteristics calculated from baseline and post-NAC at ADC<sub>all</sub> and ADC<sub>b100</sub> are presented in Supplementary Table S3. ΔADC and %ΔADC grouped by response is given in Table 2. Figure 2 summaries ΔADC seen in response groups.

The ΔADC mean was significantly greater in those achieving response with NAC compared to poor response at ΔADC<sub>all</sub> (0.32 × 10<sup>-3</sup> mm<sup>2</sup>/s versus 0.11 × 10<sup>-3</sup> mm<sup>2</sup>/s; p=0.009) and ΔADC<sub>b100</sub> (0.30 × 10<sup>-3</sup> versus 0.09 × 10<sup>-3</sup> mm<sup>2</sup>/s; p=0.007). A 21.70% increase in %ΔADC<sub>all</sub> mean was seen in response compared to the 8.23% increase in poor response (p=0.013). This corresponded to a %ΔADC<sub>b100</sub> mean increase of 25.64% in response versus 7.59% for poor response (p=0.016).

The individual AUC values calculated at baseline ADC, post-NAC ADC, ΔADC, and %ΔADC in histogram characteristics at ADC<sub>all</sub> and ADC<sub>b100</sub> are presented in Supplementary Table S4. The corresponding significant AUC cut-off criteria with associated sensitivity, specificity, PPV, and NPV are presented in Table 3.

No baseline ADC parameter was significantly associated with NAC response. Significant AUC values associated with NAC response was identified at both ADC<sub>all</sub> and ADC<sub>b100</sub> for ADC mean, 50th, 75th, and 90th percentiles of post-NAC ADC and ΔADC, and at ADC mean, 50th, and 75th percentile of %ΔADC. The parameter that had the highest specificity in discriminating between NAC response and poor response was 75th percentile ADC (AUC, 0.8; p=0.01) (Supplementary Table S4).

ΔADC<sub>all</sub> mean of 0.18 × 10<sup>-3</sup>mm<sup>2</sup>/s and ΔADC<sub>b100</sub> mean of 0.19 × 10<sup>-3</sup>mm<sup>2</sup>/s, respectively, predicted NAC response with sensitivity of 71.1% and 65.8%, specificity of 80.0% and 90.0%, PPV of 93.1% and 96.2%, and NPV of 42.1% and 40.9%, respectively.

%ΔADC<sub>all</sub> mean and %ΔADC<sub>b100</sub> mean of 18.0% and 18.1%, respectively, predicted NAC response with sensitivity of 57.9% and 60.5%, specificity of 90.0% and 90.0%, PPV 95.7% and 95.8%, and NPV 36.0% and 37.5%, respectively.

The 75th percentile ΔADC<sub>all</sub> of 0.17 × 10<sup>-3</sup> mm<sup>2</sup>/s and %ΔADC<sub>all</sub> of 13.4% predicted NAC response with sensitivity of 84.2% and 81.6%; specificity of 80.0% and 80.0%, PPV of 94.1% and 93.9%, and NPV of 57.1% and 53.3% respectively. The 75th percentile ΔADC<sub>b100</sub> of 0.22 × 10<sup>-3</sup> mm<sup>2</sup>/s and %ΔADC<sub>b100</sub> of 15.5% predicted NAC response with sensitivity of 79.0% and 68.4%, specificity of 90.0% and 90.0%, PPV of 96.8% and 96.6%, and NPV 52.9% and 47.4%, respectively.

TABLE 2 Change in ADC histogram parameters to neo-adjuvant chemotherapy as grouped by conventional response assessment.

Parameter	ΔADC							%ΔADC change						
	Response (n = 38)			Poor response (n = 10)			p value*	Response (n = 38)			Poor response (n = 10)			p value*
	Median	Min	Max	Median	Min	Max		Median	Min	Max	Median	Min	Max	
<b>ΔADC<sub>all</sub></b>														
Mean	0.32	-0.44	1.93	0.11	-0.14	0.48	0.009	21.7	-24.83	197.42	8.23	-12.96	37.11	0.013
10 <sup>th</sup> percentile	0.12	-1.22	1.00	0.06	-0.08	0.35	0.793	10.98	-100.00	141.06	7.81	-9.94	44.7	0.793
25 <sup>th</sup> percentile	0.21	-1.51	0.99	0.04	-0.06	0.32	0.114	18.49	-100.00	137.75	4.39	-7.26	34.68	0.114
50 <sup>th</sup> percentile	0.27	-0.42	1.61	0.06	-0.07	0.34	0.008	21.85	-25.96	183.01	4.84	-7.1	31.49	0.01
75 <sup>th</sup> percentile	0.44	-0.61	2.44	0.14	-0.11	0.49	0.002	29.68	-28.62	223.23	10.32	-9.81	31.27	0.002
90 <sup>th</sup> percentile	0.65	-0.72	3.66	0.18	-0.32	0.68	0.005	37.46	-24.92	247.60	10.60	-21.55	42.89	0.011
Skew	-0.55	-9.11	2.21	-0.07	-0.97	6.42	0.077	-36.23	-194.97	772.82	-4.34	-44.74	224.52	0.035
Kurtosis	-1.67	-182.2	7.79	0.555	-0.13	1.36	0.077	-72.74	-425.82	1,685.70	12.43	-93.82	1518.58	0.045
<b>ΔADC<sub>b100</sub></b>														
Mean	0.30	-0.15	1.42	0.09	-0.21	0.045	0.007	25.64	-10.95	147.82	7.59	-21.29	43.00	0.016
10 <sup>th</sup> percentile	0.09	-1.28	0.83	0.05	-0.16	0.25	0.698	9.60	-100.00	137.50	5.33	-24.06	32.6	0.698
25 <sup>th</sup> percentile	0.12	-1.54	0.89	0.05	-0.14	0.33	0.232	12.61	-100.00	160.99	6.15	-17.44	38.68	0.222
50 <sup>th</sup> percentile	0.28	-0.17	1.09	0.06	-0.11	0.37	0.021	25.64	-10.95	147.83	5.92	-12.61	37.44	0.037
75 <sup>th</sup> percentile	0.54	-0.21	1.98	0.12	-0.14	0.52	<0.0001	34.84	-13.78	221.66	10.1	-14.03	44.25	0.002
90 <sup>th</sup> percentile	0.67	-0.32	2.44	0.17	-0.32	0.80	0.008	35.12	-17.35	208.73	11.34	-23.89	57.66	0.021
Skew	0.02	-3.35	1.19	-0.02	-2.48	0.78	0.930	-36.28	-5788.78	1,525.54	-2.23	-82.53	77.80	0.360
Kurtosis	-0.57	-50.64	4.28	-0.49	-10.39	3.14	0.608	-84.71	-1840.56	529.86	-15.60	-83.62	160.78	0.077

\*Independent sample Mann Whitney U test, p values refer to comparison between response and poor response groups. Negative values reflect a decrease from baseline. Mean and percentile ADC are given in  $\times 10^{-3}$  mm<sup>2</sup>/s. Skew and kurtosis are absolute values.

### DWI as biomarker of long-term outcome

After median follow-up of 103 months (95% CI, 63.9–141.7), 31.3% (15/48) of the patients were alive and disease free. Of the 33 patients who died, 42.4% (14/33) of deaths were attributed to bladder cancer, 30.3% (10/33) were due to other causes, and 27.3% (9/33) deaths were unknown/unverified. Median OS and time to cystectomy was 31 months (95% CI,

18.5–86.9) and 44 months (95% CI, 10.0–76.2), respectively. Overall median PFS was not assessable using the Kaplan-Meier method.

ΔADC<sub>b100</sub> mean  $>0.19 \times 10^{-3}$  mm<sup>2</sup>/s was associated with a significantly improved OS (HR, 0.42; 95% CI, 0.20–0.89; p=0.023), bCSS [HR, 0.27 (95% CI, 0.08–0.84; p=0.0240)], PFS (HR, 0.26; 95% CI, 0.09–0.79; p=0.017), and time to cystectomy (HR, 0.36; 95% CI, 0.15–0.89; p=0.0271) (Figure 3).

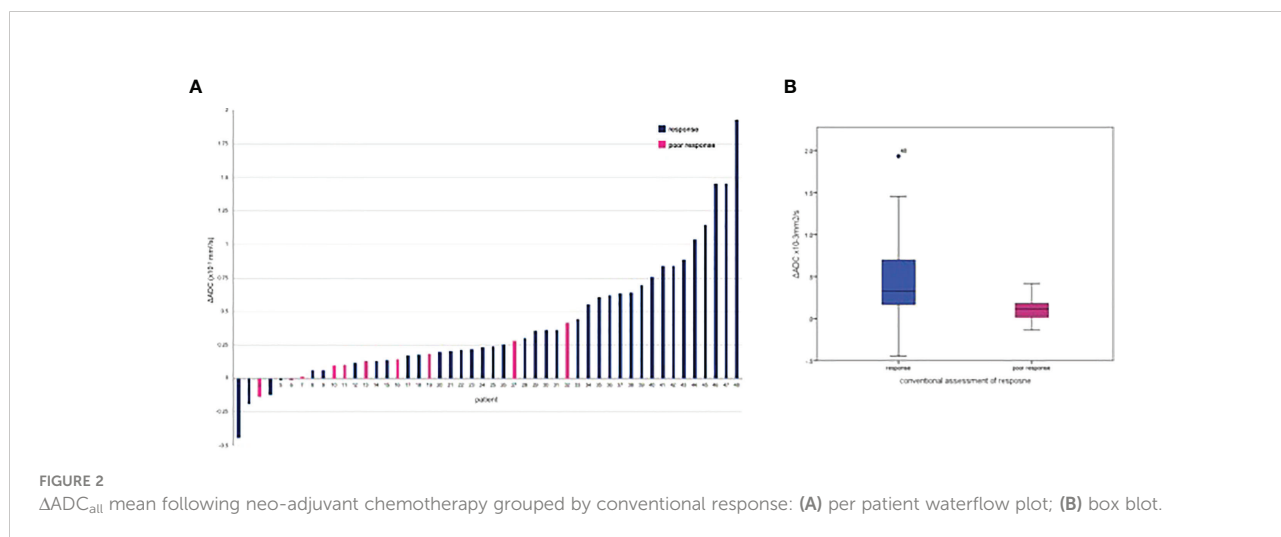


TABLE 3 Predictive power of neo-adjuvant chemotherapy response derived from significant ADC cut point parameters.

ADC parameter	ADC <sub>all</sub>									ADC <sub>b100</sub>								
	*Cut point	Sensitivity	95% CI	Specificity	95% CI	PPV	95% CI	NPV	95% CI	*Cut point	Sensitivity	95% CI	Specificity	95% CI	PPV	95% CI	NPV	95% CI
<b>Post NAC ADC (x10<sup>-3</sup> mm<sup>2</sup>/s)</b>																		
Mean	1.65	65.8	48.6 - 80.4	90.0	55.5 - 99.7	96.2	80.4 - 99.9	40.9	20.7 - 63.6	1.61	55.3	38.3 - 71.4	100.0	69.2 - 100.0	100.0	83.9 - 100.0	37.0	19.4 - 57.6
50th percentile	1.54	55.3	38.3 - 71.4	90.0	55.5 - 99.7	95.5	77.2 - 99.9	34.6	17.2 - 55.7	1.50	55.3	38.3 - 71.4	100.0	69.2 - 100.0	100.0	83.9 - 100.0	37.0	19.4 - 57.6
75th percentile	1.63	86.8	71.9 - 95.6	70.0	34.8 - 93.3	91.7	77.5 - 98.2	58.3	27.7 - 84.8	1.79	57.9	40.8 - 73.7	100.0	69.2 - 100.0	100.0	84.6 - 100.0	38.5	20.2 - 59.4
90th percentile	2.20	68.4	51.3 - 82.5	90.0	55.5 - 99.7	96.3	81.0 - 99.9	42.9	21.8 - 66.0	2.30	55.3	38.3 - 71.4	100.0	69.2 - 100.0	100.0	83.9 - 100.0	37.0	19.4 - 57.6
<b>Absolute change in ADC (x10<sup>-3</sup> mm<sup>2</sup>/s)</b>																		
Mean	0.18	71.1	54.1 - 84.6	80.0	44.4 - 97.5	93.1	77.2 - 99.2	42.1	20.3 - 66.5	0.19	65.8	48.6 - 80.4	90.0	55.5 - 99.7	96.2	80.4 - 99.9	40.9	20.7 - 63.6
50th percentile	0.18	65.8	48.6 - 80.4	90.0	55.5 - 99.7	96.2	80.4 - 99.9	40.9	20.7 - 63.6	0.11	68.4	51.3 - 82.5	80.0	44.4 - 97.5	92.9	76.5 - 99.1	40.0	19.1 - 63.9
75th percentile	0.17	84.2	68.7 - 94.0	80.0	44.4 - 97.5	94.1	80.3 - 99.3	57.1	28.9 - 82.3	0.22	79.0	62.7 - 90.4	90.0	55.5 - 99.7	96.8	83.3 - 99.9	52.9	27.8 - 77.0
90th percentile	0.68	50.0	33.4 - 66.6	100.0	69.2 - 100.0	100.0	82.4 - 100.0	34.5	17.9 - 54.3	0.50	60.5	43.4 - 76.0	90.0	55.5 - 99.7	95.8	78.9 - 99.9	37.5	18.8 - 59.4
<b>Relative percentage change in ADC</b>																		
Mean	18.0	57.9	40.8 - 73.7	90.0	55.5 - 99.7	95.7	78.1 - 99.9	36.0	18.0 - 57.5	18.1	60.5	43.4 - 76.0	90.0	55.5 - 99.7	95.8	78.9 - 99.9	37.5	18.8 - 59.4
50th percentile	16.5	60.5	43.4 - 76.0	90.0	55.5 - 99.7	95.8	78.9 - 99.9	37.5	18.8 - 59.4	8.3	68.4	51.3 - 82.5	80.0	44.4 - 97.5	92.9	76.5 - 99.1	40.0	19.1 - 63.9
75th percentile	13.4	81.6	65.7 - 92.3	80.0	44.4 - 97.5	93.9	79.8 - 99.3	53.3	26.6 - 78.7	15.5	73.7	56.9 - 86.6	90.0	55.5 - 99.7	96.6	82.2 - 99.9	47.4	24.4 - 71.1

\*Only cut points for significant AUC presented. The discriminatory threshold is greater than the cut point determined. NPV, negative predictive value; PPV, positive predictive value.

% $\Delta\text{ADC}_{b100} > 15.5\%$  at 75th percentile was associated with significant improvement in OS (HR, 0.40; 95% CI, 0.19–0.86;  $p=0.0179$ ), bCSS (HR, 0.26; 95% CI, 0.08–0.82;  $p=0.0214$ ), PFS (HR, 0.16; 95% CI, 0.05–0.48;  $p=0.0012$ ), and time to cystectomy (HR, 0.19; 95% CI, 0.07–0.47;  $p=0.0004$ ) (Figure 3). A summary of all time to event outcomes according to the derived imaging biomarkers is given in Supplementary Table S5.

## Discussion

Risk stratification is critical for personalising MIBC follow-up schedules, safely selecting candidates for bladder preservation protocols, and identifying poor prognosis disease who could benefit from treatment intensification following NAC. We presented first quantitative DWI analysis to both successfully determine NAC response and survival outcomes in localised MIBC. It provides supporting evidence that imaging biomarkers could be non-invasive tools for NAC assessment and means of determining NAC sensitivity. Quantitative imaging biomarkers may therefore provide adjunct to molecular predictors currently being investigated (8).

Liquid-biopsy-derived biomarkers from plasma or urine do not present threat to imaging biomarkers but are likely to compliment predictive and prognostic power (8, 32–34). Circulating tumour DNA (ctDNA) can be detected in most patients with metastatic bladder but has attenuated sensitivity in those with localised organ-confined disease. ctDNA bladder cancer detection rates fall from 73% in metastatic disease to 14% in organ-confined disease (35–37). However, ctDNA presence prior to NAC, dynamics during NAC, and detection at follow-up provide prognostic information (38). The detection of urinary bladder cancer associated mutations has been evaluated in the context of diagnosis and non-muscle-invasive bladder cancer surveillance (39, 40). Their role in predicting NAC response is yet to be determined.

A perceived study drawback may be that NAC response was not defined pathologically in all our patients. Biopsy or TURBT was not always undertaken if there was obvious presence or absence of tumour at cystoscopy that would not have altered the patient's preferred definitive treatment choice. When performed, its limitation in diagnostic accuracy to assess true residual disease following NAC is acknowledged (41). In a series of 114 patients who underwent TURBT following NAC and then proceeded to radical cystectomy, Becker et al. demonstrated that 32% of patients were falsely downstaged as compared to their final pathology, which demonstrated residual MIBC ( $\geq\text{ypT2}$ ). Subset analysis of this series demonstrated that 81% (17/21) who had no residual disease visible on cystoscopy were T0 at TURBT, with 24% (4/21) having  $\geq\text{ypT2}$  at cystectomy (41). It is also recognised that pCR remains a surrogate endpoint with limitations when evaluating neoadjuvant therapies in MIBC (42). Arguably, we have therefore presented a more direct

measure of clinical relevance with the corresponding time to survival event endpoint analyses.

The study protocol precedes VI-RADS image acquisition recommendation (17). Nevertheless, many of the technical considerations made therein were used in the study protocol, as the authors contributed to VI-RADS development. VI-RADS mpMRI qualitative scoring is used to aid pre-treatment staging, but its application on the assessment of treatment response is yet to be determined.

Qualitative DWI response reporting appears reliant on expertise. Although inter-reader agreement is good in the diagnostic setting (43), identifying complete treatment response is subject to greater reporting variation (44). Quantitative image analysis, therefore, has the potential to overcome reporting discrepancy.

ADC was calculated and presented using all b-values of 0–750  $\text{s/mm}^2$  ( $\text{ADC}_{\text{all}}$ ) and high b-values of 100–750  $\text{s/mm}^2$  ( $\text{ADC}_{b100}$ ). Biophysical processes such as blood flow and perfusion can increase apparent water mobility and adversely impact on accurately measuring tissue water diffusion. The use of high b-values can suppress these contributing effects (45). The significant difference seen at baseline between mean  $\text{ADC}_{\text{all}}$  and mean  $\text{ADC}_{b100}$  illustrates the magnitude of perfusion effects and reflects the intrinsic vascularity of bladder tumours (28). It highlights the importance of selecting appropriate b-values for ADC calculation and for quantitative DWI biomarker development in these circumstances.

Given that ADC estimates depend on the chosen b-values, direct comparison of absolute ADC values between studies with differing acquisition protocols should be avoided (28). Similarly, the specific ADC thresholds defined in this study relate to the decreasing cellular density associated with NAC response and are unlikely to be directly applicable to assess response with other treatment modalities. For example, stromal tissue effector cell infiltration seen with immunotherapy response is cited as the potential reason why quantitative ADC assessment was unreliable in assessing neoadjuvant pembrolizumab response within the PURE-01 study (44).

No measured pre-treatment baseline ADC feature could successfully identify NAC outcome. A potential confounding factor is the time variation from initial diagnostic TURBT to baseline MRI, as the degree of post-procedural inflammation and oedema could have impacted on the diffusion characteristics of the absolute baseline ADC reading (28). Repeatability of baseline ADC is estimated to be approximately 15%; therefore, any increase following treatment greater than this can be considered real (46). It is therefore expected that the ADC difference between good tumour response and poor response is larger than the variation caused by inflammation, oedema, and fibrosis caused by artefact post-TURBT.

Another likely contributing factor impacting on the predictive potential of the baseline MRI is vendor variation; 54.2% (26/48) of baseline MRI scans were performed on the

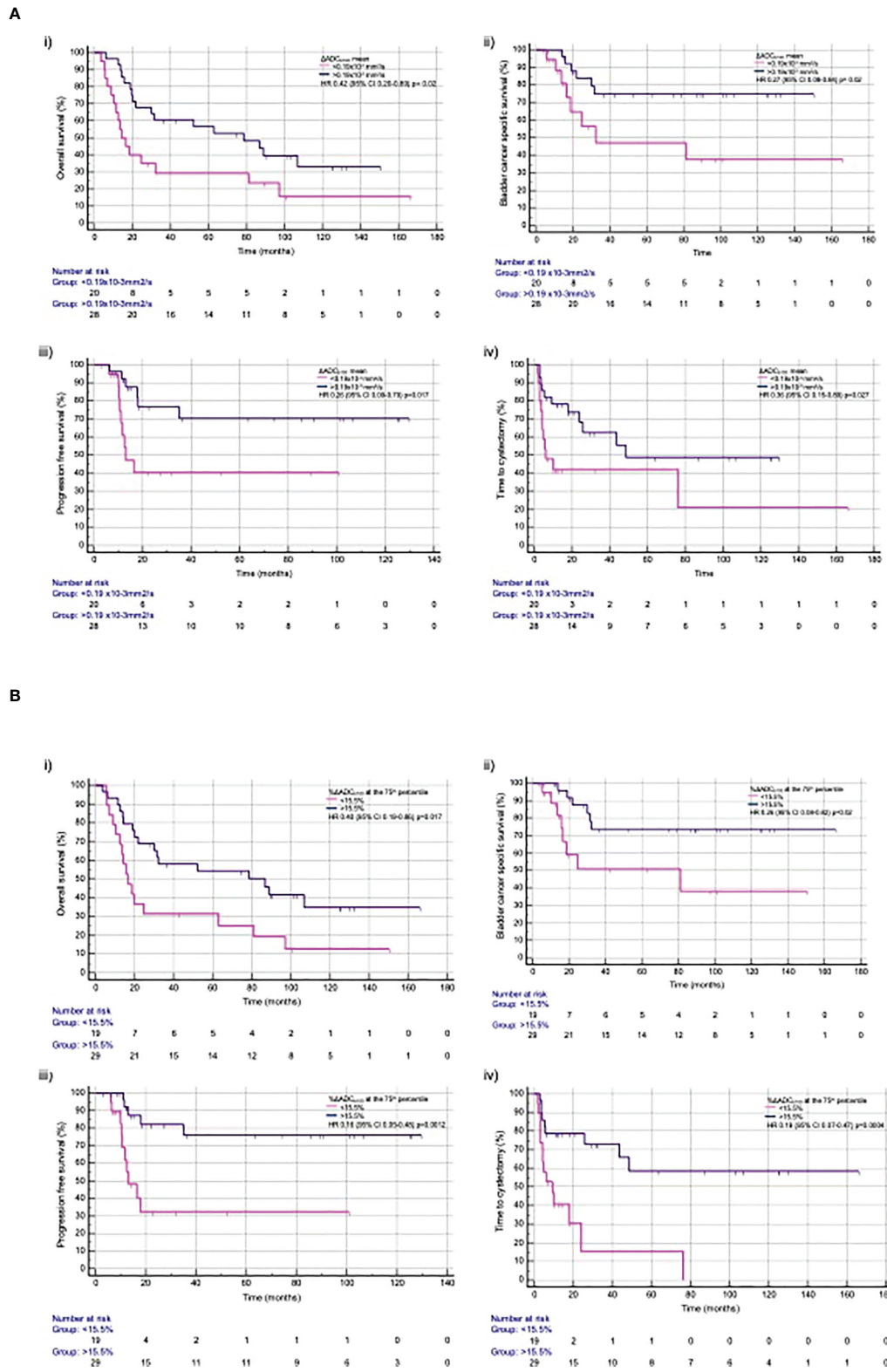


**FIGURE 3** Time to event outcomes with (A)  $\Delta ADC_{b100}$  mean and (B)  $\% \Delta ADC_{b100}$  at the 75th percentile for (i) overall survival, (ii) bladder cancer specific free survival, (iii) progression-free survival, and (iv) time to cystectomy.

Intera system, 39.6% (19/48) on the Aera system, and 6.3% (3/48) on the Avanto system. *Post-hoc* analysis provided in [Supplementary Material 1](#) identified that the baseline mean ADC calculation was statistically significant between the Intera and Aera systems. Importantly, however, only three patients had a scanner/vendor switch at their post-NAC MRI. Therefore, individual patients provided internal control of this variable when  $\Delta$ ADC was considered. The measured  $\Delta$ ADC between the vendors was not statistically significant, and the  $\Delta$ ADC was large enough to mitigate scanner differences.

Although no baseline ADC characteristic could determine NAC response, scanning earlier during NAC may help provide this information. A feasibility study of 16 patients demonstrated change in mean ADC after cycles 1 and 2 of NAC-predicted final response (46). Early prediction of final chemotherapy response has also been demonstrated after two cycles in those with more advanced disease using DCE (47). We have expanded our current protocol to include scanning following cycle 1 to determine whether earlier quantitative signal can be successfully identified.

Additional predictive potential may come from considering alternative DWI analysis. In this study, ADC was derived by fitting a mono-exponential function. However, in other tumours, this model does not fully describe the DWI signal (48). Alternative models have been applied to better describe tumour behaviour (49–51). Radiomic feature extraction from the MRI data may also add to predictive power (52). Textural features derived from DWI and ADC maps can predict bladder tumour grade and muscle-invasive disease (53–55). Its application in bladder cancer treatment response prediction remains novel.

A proportion of the patients were deemed non-evaluable at baseline because no identifiable DWI signal was seen at initial scan following TURBT. In the current standard MIBC diagnostic paradigm wedded to TURBT for T staging, universal utility of an imaging biomarker to predict NAC response is likely to be limited. The BladderPath Trial (ISRCTN 35296862) will help determine safety of an mpMRI-directed diagnostic pathway in MIBC (56). It is anticipated that this study will inform if patients with high likelihood of MIBC based on mpMRI and tumour biopsy alone can safely proceed to treatment without TURBT. If successful, it would make DWI-derived biomarker to assess treatment response more widely applicable.

Before the defined DWI biomarkers can be tested within clinical trials to inform treatment decision-making, technical validation to assess reproducibility and repeatability in the multi-centre setting is required (9). This work is planned. We envisaged that quantitative DWI biomarkers will be used in the future as part of the qualifying criteria for bladder preservation following NAC alongside various DDR mutations and cell cycle

and regulatory genes that are currently being evaluated in prospective studies.

## Conclusion

We present first quantitative DWI analysis to both successfully determine NAC response and provide prognostic information regarding long-term clinical MIBC outcomes following NAC. Multi-centre validation to assess reproducibility and repeatability is required before testing within clinical trials to inform MIBC treatment decision-making.

## Data availability statement

The datasets presented in this article are not readily available. The Data and Sample Access Policy is available on our external facing web pages. Priority will be given to projects from within the original study proposal and access will usually be reserved for study purposes until those studies are concluded. Data and/or samples will not be released where this could impact on the reporting of on-going research questions of the study. Requests to access the datasets should be directed to [shaista.hafeez@icr.ac.uk](mailto:shaista.hafeez@icr.ac.uk).

## Ethics statement

This study was reviewed and approved by The Royal Marsden NHS Foundation Trust. The patients/participants provided their written informed consent to participate in this study.

## Author contributions

All authors meet at least one the criteria recommended by the IJCME. SH performed the analysis and wrote the first draft of the manuscript. All authors contributed to the article and approved the submitted version.

## Funding

The authors acknowledge this study represents independent research supported by the National Institute for Health Research (NIHR) Biomedical Research Centre at The Royal Marsden NHS Foundation Trust and The Institute of Cancer Research, London. The views expressed are those of the author(s) and not necessarily those of the NIHR or the Department of Health and Social Care. The work was supported by Cancer Research UK programme grant (C33589/A19727 and C33589/A28284).

## Conflict of interest

The authors declare that the research was conducted in the absence of any commercial or financial relationships that could be construed as a potential conflict of interest.

## Publisher's note

All claims expressed in this article are solely those of the authors and do not necessarily represent those of their affiliated

organizations, or those of the publisher, the editors and the reviewers. Any product that may be evaluated in this article, or claim that may be made by its manufacturer, is not guaranteed or endorsed by the publisher.

## Supplementary material

The Supplementary Material for this article can be found online at: <https://www.frontiersin.org/articles/10.3389/fonc.2022.961393/full#supplementary-material>

## References

- Witjes JA, Bruins HM, Cathomas R, Comperat EM, Cowan NC, Gakis G, et al. European Association of urology guidelines on muscle-invasive and metastatic bladder cancer: Summary of the 2020 guidelines. *Eur Urol* (2021) 79(1):82–104. doi: 10.1016/j.eururo.2020.03.055
- James ND, Hussain SA, Hall E, Jenkins P, Tremlett J, Rawlings C, et al. Radiotherapy with or without chemotherapy in muscle-invasive bladder cancer. *N Engl J Med* (2012) 366(16):1477–88. doi: 10.1056/NEJMoa1106106
- Hoskin PJ, Rojas AM, Bentzen SM, Saunders MI. Radiotherapy with concurrent carbogen and nicotinamide in bladder carcinoma. *J Clin Oncol* (2010) 28(33):4912–8. doi: 10.1200/JCO.2010.28.4950
- National Institute for Health and Clinical Excellence (NICE) Guidance. *Bladder cancer: diagnosis and management* (2015). Available at: <http://www.nice.org.uk/guidance/ng2/evidence/full-guideline-3744109>.
- Advanced Bladder Cancer Meta-analysis C. Neoadjuvant chemotherapy in invasive bladder cancer: update of a systematic review and meta-analysis of individual patient data advanced bladder cancer (ABC) meta-analysis collaboration. *Eur Urol* (2005) 48(2):202–5. doi: 10.1016/j.eururo.2005.04.006
- Yin M, Joshi M, Meijer RP, Glantz M, Holder S, Harvey HA, et al. Neoadjuvant chemotherapy for muscle-invasive bladder cancer: A systematic review and two-step meta-analysis. *Oncologist* (2016) 21(6):708–15. doi: 10.1634/theoncologist.2015-0440
- Kamoun A, de Reynies A, Allory Y, Sjodahl G, Robertson AG, Seiler R, et al. A consensus molecular classification of muscle-invasive bladder cancer. *Eur Urol* (2020) 77(4):420–33. doi: 10.1016/j.eururo.2019.09.006
- Motterle G, Andrews JR, Morlacco A, Karnes RJ. Predicting response to neoadjuvant chemotherapy in bladder cancer. *Eur Urol Focus* (2020) 6(4):642–9. doi: 10.1016/j.euf.2019.10.016
- O'Connor JP, Aboagye EO, Adams JE, Aerts HJ, Barrington SF, Beer AJ, et al. Imaging biomarker roadmap for cancer studies. *Nat Rev Clin Oncol* (2017) 14(3):169–86. doi: 10.1038/nrclinonc.2016.162
- Gandhi N, Krishna S, Booth CM, Breau RH, Flood TA, Morgan SC, et al. Diagnostic accuracy of magnetic resonance imaging for tumour staging of bladder cancer: systematic review and meta-analysis. *BJU Int* (2018) 122(5):744–53. doi: 10.1111/bju.14366
- Woo S, Suh CH, Kim SY, Cho JY, Kim SH. Diagnostic performance of MRI for prediction of muscle-invasiveness of bladder cancer: A systematic review and meta-analysis. *Eur J Radiol* (2017) 95:46–55. doi: 10.1016/j.ejrad.2017.07.021
- Huang L, Kong Q, Liu Z, Wang J, Kang Z, Zhu Y. The diagnostic value of MR imaging in differentiating T staging of bladder cancer: A meta-analysis. *Radiology* (2018) 286(2):502–11. doi: 10.1148/radiol.2017171028
- Kulkarni GS, Hakenberg OW, Gschwend JE, Thalmann G, Kassouf W, Kamat A, et al. An updated critical analysis of the treatment strategy for newly diagnosed high-grade T1 (previously T1G3) bladder cancer. *Eur Urol* (2010) 57(1):60–70. doi: 10.1016/j.eururo.2009.08.024
- Klaassen Z, Kamat AM, Kassouf W, Gontero P, Villavicencio H, Bellmunt J, et al. Treatment strategy for newly diagnosed T1 high-grade bladder urothelial carcinoma: New insights and updated recommendations. *Eur Urol* (2018) 74(5):597–608. doi: 10.1016/j.eururo.2018.06.024
- Gray PJ, Lin CC, Jemal A, Shipley WU, Fedewa SA, Kibel AS, et al. Clinical-pathologic stage discrepancy in bladder cancer patients treated with radical cystectomy: results from the national cancer data base. *Int J Radiat Oncol Biol Phys* (2014) 88(5):1048–56. doi: 10.1016/j.ijrobp.2014.01.001
- Paik ML, Scolieri MJ, Brown SL, Spirnak JP, Resnick MI. Limitations of computerized tomography in staging invasive bladder cancer before radical cystectomy. *J Urol* (2000) 163(6):1693–6. doi: 10.1016/S0022-5347(05)67522-2
- Panebianco V, Narumi Y, Altun E, Bochner BH, Efstathiou JA, Hafeez S, et al. Multiparametric magnetic resonance imaging for bladder cancer: Development of VI-RADS (Vesical imaging-reporting and data system). *Eur Urol* (2018) 74(3):294–306. doi: 10.1016/j.eururo.2018.04.029
- Yoshida S, Koga F, Kobayashi S, Ishii C, Tanaka H, Tanaka H, et al. Role of diffusion-weighted magnetic resonance imaging in predicting sensitivity to chemoradiotherapy in muscle-invasive bladder cancer. *Int J Radiat Oncol Biol Phys* (2012) 83(1):e21–27. doi: 10.1016/j.ijrobp.2011.11.065
- Kobayashi S, Koga F, Kajino K, Yoshita S, Ishii C, Tanaka H, et al. Apparent diffusion coefficient value reflects invasive and proliferative potential of bladder cancer. *J Magn Reson Imaging* (2014) 39(1):172–8. doi: 10.1002/jmri.24148
- Sevcenco S, Ponthold L, Heinz-Peer G, Fajkovic H, Haitel A, Susani M, et al. Prospective evaluation of diffusion-weighted MRI of the bladder as a biomarker for prediction of bladder cancer aggressiveness. *Urol Oncol* (2014) 32(8):1166–71. doi: 10.1016/j.urolonc.2014.04.019
- Kobayashi S, Koga F, Yoshida S, Masuda H, Ishii C, Tanaka H, et al. Diagnostic performance of diffusion-weighted magnetic resonance imaging in bladder cancer: potential utility of apparent diffusion coefficient values as a biomarker to predict clinical aggressiveness. *Eur Radiol* (2011) 21(10):2178–86. doi: 10.1007/s00330-011-2174-7
- Takeuchi M, Sasaki S, Ito M, Okada S, Takahashi S, Kawai T, et al. Urinary bladder cancer: diffusion-weighted MR imaging—accuracy for diagnosing T stage and estimating histologic grade. *Radiology* (2009) 251(1):112–21. doi: 10.1148/radiol.25111080873
- Hafeez S, Huddart R. Advances in bladder cancer imaging. *BMC Med* (2013) 11:104. doi: 10.1186/1741-7015-11-104
- Yoshida S, Koga F, Kawakami S, Ishii C, Tanaka H, Numao N, et al. Initial experience of diffusion-weighted magnetic resonance imaging to assess therapeutic response to induction chemoradiotherapy against muscle-invasive bladder cancer. *Urology* (2010) 75(2):387–91. doi: 10.1016/j.urology.2009.06.111
- Kyriazi S, Collins DJ, Messiou C, Pennert K, Davidson RL, Giles SL, et al. Metastatic ovarian and primary peritoneal cancer: assessing chemotherapy response with diffusion-weighted MR imaging—value of histogram analysis of apparent diffusion coefficients. *Radiology* (2011) 261(1):182–92. doi: 10.1148/radiol.11110577
- Cui Y, Zhang XP, Sun YS, Tang L, Shen L. Apparent diffusion coefficient: potential imaging biomarker for prediction and early detection of response to chemotherapy in hepatic metastases. *Radiology* (2008) 248(3):894–900. doi: 10.1148/radiol.2483071407
- Harry VN, Semple SI, Gilbert FJ, Parkin DE. Diffusion-weighted magnetic resonance imaging in the early detection of response to chemoradiation in cervical cancer. *Gynecol Oncol* (2008) 111(2):213–20. doi: 10.1016/j.ygyno.2008.07.048
- Padhani AR, Liu G, Mu-Koh D, Chenvert TL, Thoeny HC, Takahara T, et al. Diffusion-weighted magnetic resonance imaging as a cancer biomarker: Consensus and recommendations. *Neoplasia* (2009) 11(2):102–25. doi: 10.1593/neo.81328

29. Ahmed SA, Taher MGA, Ali WA, Ebrahim M. Diagnostic performance of contrast-enhanced dynamic and diffusion-weighted MR imaging in the assessment of tumor response to neoadjuvant therapy in muscle-invasive bladder cancer. *Abdominal Radiol (New York)* (2021) 46(6):2712–21. doi: 10.1007/s00261-021-02963-7
30. Hafeez S, Horwich A, Omar O, Mohammed K, Thompson A, Kumar P, et al. Selective organ preservation with neo-adjuvant chemotherapy for the treatment of muscle invasive transitional cell carcinoma of the bladder. *Br J Cancer* (2015) 112(10):1626–35. doi: 10.1038/bjc.2015.109
31. Johnson W, Taylor MB, Carrington BM, Bonington SC, Swindell R. The value of hyoscine butylbromide in pelvic MRI. *Clin Radiol* (2007) 62(11):1087–93. doi: 10.1016/j.crad.2007.05.007
32. Ferro M, La Civita E, Liotti A, Cennamo M, Tortora F, Buonerba C, et al. Liquid biopsy biomarkers in urine: A route towards molecular diagnosis and personalized medicine of bladder cancer. *J Pers Med* (2021) 11(3). doi: 10.3390/jpm11030237
33. Ward DG, Bryan RT. Liquid biopsies for bladder cancer. *Transl Androl Urol* (2017) 6(2):331–5. doi: 10.21037/tau.2017.03.08
34. Birkenkamp-Demtroder K, Nordentoft I, Christensen E, Hoyer S, Reinert T, Vang S, et al. Genomic alterations in liquid biopsies from patients with bladder cancer. *Eur Urol* (2016) 70(1):75–82. doi: 10.1016/j.eururo.2016.01.007
35. Vandekerckhove G, Todenhofer T, Annala M, Struss WJ, Wong A, Beja K, et al. Circulating tumor DNA reveals clinically actionable somatic genome of metastatic bladder cancer. *Clin Cancer Res* (2017) 23(21):6487–97. doi: 10.1158/1078-0432.CCR-17-1140
36. Barata PC, Koshkin VS, Funchain P, Sohal D, Pritchard A, Klek S, et al. Next-generation sequencing (NGS) of cell-free circulating tumor DNA and tumor tissue in patients with advanced urothelial cancer: a pilot assessment of concordance. *Ann Oncol* (2017) 28(10):2458–63. doi: 10.1093/annonc/mdx405
37. Chalfin HJ, Glavaris SA, Gorin MA, Kates MR, Fong MH, Dong L, et al. Circulating tumor cell and circulating tumor DNA assays reveal complementary information for patients with metastatic urothelial cancer. *Eur Urol Oncol* (2021) 4(2):310–4. doi: 10.1016/j.euo.2019.08.004
38. Christensen E, Birkenkamp-Demtröder K, Sethi H, Shchegrova S, Salari R, Nordentoft I, et al. Early detection of metastatic relapse and monitoring of therapeutic efficacy by ultra-deep sequencing of plasma cell-free DNA in patients with urothelial bladder carcinoma. *J Clin Oncol* (2019) 37(18):1547–57. doi: 10.1200/JCO.18.02052
39. Ward DG, Baxter L, Ott S, Gordon NS, Wang J, Patel P, et al. Highly sensitive and specific detection of bladder cancer via targeted ultra-deep sequencing of urinary DNA. *Eur Urol Oncol* (2022). doi: 10.1016/j.euo.2022.03.005
40. Ward DG, Gordon NS, Boucher RH, Pirrie SJ, Baxter L, Ott S, et al. Targeted deep sequencing of urothelial bladder cancers and associated urinary DNA: a 23-gene panel with utility for non-invasive diagnosis and risk stratification. *BJU Int* (2019) 124(3):532–44. doi: 10.1111/bju.14808
41. Becker REN, Meyer AR, Brant A, Reese AC, Biles MJ, Harris KT, et al. Clinical restaging and tumor sequencing are inaccurate indicators of response to neoadjuvant chemotherapy for muscle-invasive bladder cancer. *Eur Urol* (2021) 79(3):364–71. doi: 10.1016/j.eururo.2020.07.016.7
42. Chang E, Apolo AB, Bangs R, Chisolm S, Duddalwar V, Efstathiou JA, et al. Refining neoadjuvant therapy clinical trial design for muscle-invasive bladder cancer before cystectomy: a joint US food and drug administration and bladder cancer advocacy network workshop. *Nat Rev Urol* (2022) 19(1):37–46. doi: 10.1038/s41585-021-00505-w
43. Segulier D, Puech P, Kool R, Dermis L, Gabert H, Kassouf W, et al. Multiparametric magnetic resonance imaging for bladder cancer: a comprehensive systematic review of the vesical imaging-reporting and data system (VI-RADS) performance and potential clinical applications. *Ther Adv Urol* (2021) 13:17562872211039583. doi: 10.1177/17562872211039583
44. Necchi A, Bandini M, Calareso G, Raggi D, Pederzoli F, Fare E, et al. Multiparametric magnetic resonance imaging as a noninvasive assessment of tumor response to neoadjuvant pembrolizumab in muscle-invasive bladder cancer: Preliminary findings from the PURE-01 study. *Eur Urol* (2020) 77(5):636–43. doi: 10.1016/j.eururo.2019.12.016
45. Yoshida S, Koga F, Kobayashi S, Tanaka H, Satoh S, Fujii Y, et al. Diffusion-weighted magnetic resonance imaging in management of bladder cancer, particularly with multimodal bladder-sparing strategy. *World J Radiol* (2014) 6(6):344–54. doi: 10.4329/wjrv.v6.i6.344
46. Pearson RA, Thelwall PE, Snell J, McKenna J, Pieniazek P, Fitzgerald EL, et al. Evaluation of early response to neoadjuvant chemotherapy in muscle-invasive bladder cancer using dynamic contrast-enhanced MRI and diffusion weighted MRI: MARBLE study. *J Clin Oncol* (2016) 34(2\_suppl):403–3. doi: 10.1200/jco.2016.34.2\_suppl.403
47. Schrier BP, Peters M, Barentsz JO, Witjes JA. Evaluation of chemotherapy with magnetic resonance imaging in patients with regionally metastatic or unresectable bladder cancer. *Eur Urol* (2006) 49(4):698–703. doi: 10.1016/j.eururo.2006.01.022
48. Sala E, Priest AN, Kataoka M, Graves MJ, McLean MA, Joubert I, et al. Apparent diffusion coefficient and vascular signal fraction measurements with magnetic resonance imaging: feasibility in metastatic ovarian cancer at 3 Tesla: technical development. *Eur Radiol* (2010) 20(2):491–6. doi: 10.1007/s00330-009-1543-y
49. Winfield JM, deSouza NM, Priest AN, Wakefield JC, Hodgkin C, Freeman S, et al. Modelling DW-MRI data from primary and metastatic ovarian tumours. *Eur Radiol* (2015) 25(7):2033–40. doi: 10.1007/s00330-014-3573-3
50. Orton MR, Collins DJ, Koh DM, Leach MO. Improved intravoxel incoherent motion analysis of diffusion weighted imaging by data driven Bayesian modeling. *Magn Reson Med* (2014) 71(1):411–20. doi: 10.1002/mrm.24649
51. Taouli B, Beer AJ, Chenevert T, Collins D, Lehman C, Matos C, et al. Diffusion-weighted imaging outside the brain: Consensus statement from an ISMRM-sponsored workshop. *J Magn Reson Imaging* (2016) 44(3):521–40. doi: 10.1002/jmri.25196
52. Aerts HJ, Velazquez ER, Leijenaar RT, Parmar C, Grossmann P, Carvalho S, et al. Decoding tumour phenotype by noninvasive imaging using a quantitative radiomics approach. *Nat Commun* (2014) 5:4006. doi: 10.1038/ncomms5006
53. Zhang X, Xu X, Tian Q, Li B, Wu Y, Yang Z, et al. Radiomics assessment of bladder cancer grade using texture features from diffusion-weighted imaging. *J Magn Reson Imaging* (2017) 46(5):1281–88. doi: 10.1002/jmri.25669
54. Huang X, Wang X, Lan X, Deng J, Lei Y, Lin F. The role of radiomics with machine learning in the prediction of muscle-invasive bladder cancer: A mini review. *Front Oncol* (2022) 12. doi: 10.3389/fonc.2022.990176
55. Zheng Z, Xu F, Gu Z, Yan Y, Xu T, Liu S, et al. Combining multiparametric MRI radiomics signature with the vesical imaging-reporting and data system (VI-RADS) score to preoperatively differentiate muscle invasion of bladder cancer. *Front Oncol* (2021) 11. doi: 10.3389/fonc.2021.619893
56. Bryan RT, Liu W, Pirrie SJ, Amir R, Gallagher J, Hughes AI, et al. Comparing an imaging-guided pathway with the standard pathway for staging muscle-invasive bladder cancer: Preliminary data from the BladderPath study. *Eur Urol* (2021) 80(1):12–5. doi: 10.1016/j.eururo.2021.02.021